Alloying effect on $K\beta$-to-$K\alpha$ intensity ratios in Ti_xNi_{1-x} and Cr_xNi_{1-x} alloys studied by γ-ray fluorescence and fast proton ionization

C. R. Bhuinya and H. C. Padhi
Institute of Physics, Bhubaneswar, India
(Received 11 February 1992; revised manuscript received 29 December 1992)

K x-ray intensity ratios in Ti_xNi_{1-x} and Cr_xNi_{1-x} alloys have been measured for different compositions x, using 59.54-keV γ-ray fluorescence (γRF) and 4.07-MeV-proton ionization. The intensity ratios were found to be higher than those of pure metal values for Ti in Ti_xNi_{1-x} alloys for $x=0.35$ and for Cr in Cr_xNi_{1-x} alloys for $x=0.20$. The γRF results are supported by the proton-induced x-ray emission (PIXE) results for all the constituent metals of both the alloys. The results are discussed on the basis of $3d$-electron transfer or rearrangement in the individual metals of corresponding alloys.

PACS number(s): 32.70.Fw

I. INTRODUCTION

The purpose of this paper is to present the data on the measurement of the $K\beta$-to-$K\alpha$ intensity ratios (hereafter called R) of Ti, Cr, and Ni in Ti_xNi_{1-x} and Cr_xNi_{1-x} alloys for different compositions x, which clearly indicate deviation of R for Ti and Cr in certain alloy compositions from those obtained for the pure metals. In our earlier work [1], we have discussed in detail the γ-ray-fluorescence (γRF) results obtained from Cr_xNi_{1-x} alloys together with those obtained from pure Cr and Ni metals. This experiment resulted in a significant deviation ($\sim 18\%$) in the R value of Cr in the $Cr_{0.2}Ni_{0.8}$ alloy from that of the pure-Cr metal value, which inspired us to investigate the phenomena in more detail. So, we repeated the work in Cr_xNi_{1-x} alloys using a 4.07-MeV proton beam, and its results supported our earlier γRF results. Also, γRF and proton-induced x-ray emission (PIXE) results agree with each other within error. Then the same type of work has been carried out in Ti_xNi_{1-x} alloys using both γRF and PIXE methods. The R values in Ti_xNi_{1-x} alloys show a similar trend as in the case of Cr_xNi_{1-x} alloys. Although for the Cr_xNi_{1-x} alloys the γRF and PIXE results are somewhat closer to each other, in Ti_xNi_{1-x} we observe an enhancement in the ratio R of titanium, which may be due to some systematic errors in the background correction for the PIXE data. Although multivacancy production for various metals was seen earlier by Li and Watson [2] for carbon projectiles, they did not see it for deuteron and α particles.

Earlier magnetization measurements [3] and Compton-profile studies [4,5] of these alloys suggested that there is electron transfer or rearrangement when Ti and Cr metals are alloyed with nickel. In this work, we want to show that the $K\beta$-to-$K\alpha$ intensity ratios can be used as a sensitive tool to study such electron-transfer or -rearrangement phenomena in alloys. To our knowledge, this type of measurements in alloys has not been previously reported.

II. EXPERIMENT

The experimental setups for γRF and PIXE measurements have been described in detail in our earlier works [1,6]. The pure metal samples were in the form of thick foils (thickness ~ 0.5 mm), and most of the alloy compositions were in the form of powders, which were pressed into pellets of thickness ~ 1 mm. All the samples were procured from Good Fellow Company, U.K.

A. Experiment with γ-ray source

The samples were irradiated with a 200-mCi ^{241}Am γ-ray source with γ-ray energy of 59.54 keV. The fluorescent x rays were detected with a 33-mm$^2\times$5-mm Si(Li) detector. The Si(Li) detector has a 12.5-μm-thick beryllium window and is sealed inside the cryostat. The γ-ray source was shielded from the Si(Li) detector using a lead shield cum collimator assembly. A schematic diagram of the experimental setup is shown in Fig. 1.

The preamplifier pulses from the Si(Li) detector were fed to an ORTEC-572 model spectroscopy amplifier and were then analyzed by a ND-62 multichannel analyzer. Electronics drift in the counting system was controlled with the help of a ND-2000 digital spectrum stabilizer tagged to the pulser peak of an ORTEC-448 research pulser. The gain of the system was maintained at 30 eV/channel. The resolution of the Si(Li) detector was ~ 170 eV [full width at half maximum (FWHM)] for a

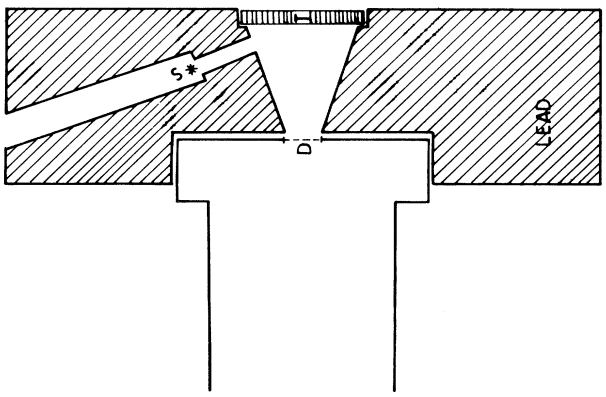

FIG. 1. Schematic diagram of the γ-ray fluorescence. Setup, *S*: ^{142}Am source; *D*: Si(Li) detector; *T*: target.

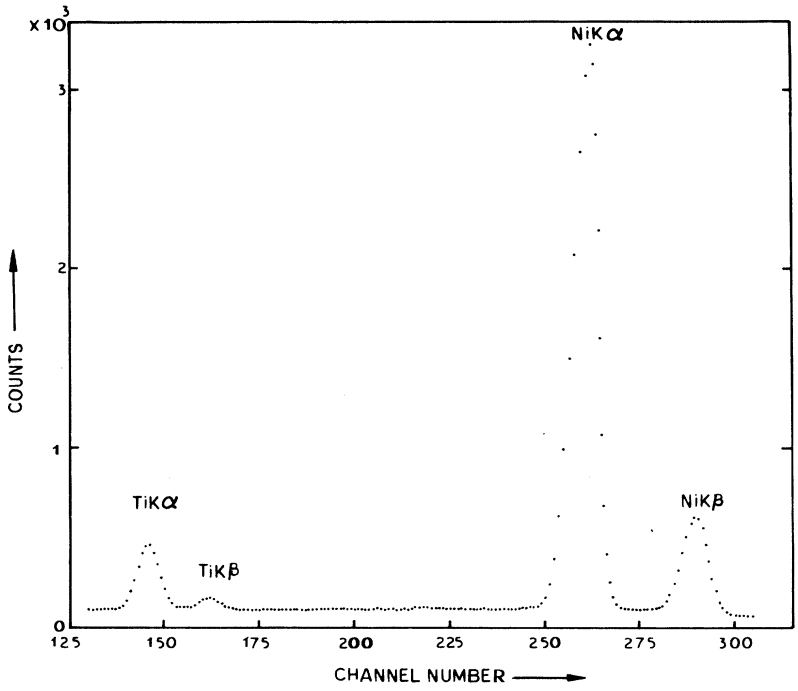

FIG. 2. K x-ray spectrum of $Ti_{0.35}Ni_{0.65}$ alloy obtained by 59.4-KeV γ-ray fluorescence experiment.

5.9-keV x-ray peak. The counting was continued until counts under the less intense $K\beta$ peak were around 4×10^4 counts. A sample K x-ray spectrum for $Ti_{0.35}N_{0.65}$ alloy is shown in Fig. 2.

B. Experiment with proton beam

In this case, the samples were irradiated with a 4.07-MeV proton beam from the 3-MV 9SDH-2 tandem pelletron accelerator. H^- ions from a cesium sputtered negative-ion source (SNICS) were preaccelerated by $\sim$70 kV voltage, and then injected into the main accelerating column with the help of an injector magnet. At the terminal, the H^- ions were charge exchanged using nitrogen as a stripper gas to obtain H^+ ions, which were further accelerated by the terminal voltage to obtain the desired energy. After the acceleration, the proton beam was momentum analyzed with the help of a 90° analyzing magnet. The analyzed beam was then switched to the 45° beamline with the help of a seven-port switching magnet. Finally the beam was focused, with the help of a magnetic-quadrupole doublet onto the target through a graphite collimator of $\sim$1.5-mm aperture located at $\sim$10 cm before the target. The targets were mounted on a stainless-steel ladder having the facility for mounting four targets at a time. The samples were held in position by aluminum cover plates (0.75 mm thick) having a 1-cm hole at the center for the beam to pass through. Use of aluminum covers helps in reducing the background in the spectral region of interest. A schematic diagram of the experimental setup is shown in Fig. 3.

Before starting any experimental run for spectrum collection, the beam was adjusted at the center of a quartz plate fixed in one of the ladder positions. Then the sample was brought into beam position by sliding the target ladder by an appropriate length measured with the help of an outside scale. The target was placed at an angle of 45° to the beam direction. The Si(Li) detector that was used during γRF measurements was kept at an angle of 90° to the beam direction and was facing the target at an angle of 45° through a 3.5-mg/cm^2-thick aluminized Mylar window. The Si(Li) detector was at a distance of 10 cm from the target. The exposed target diameter was 10

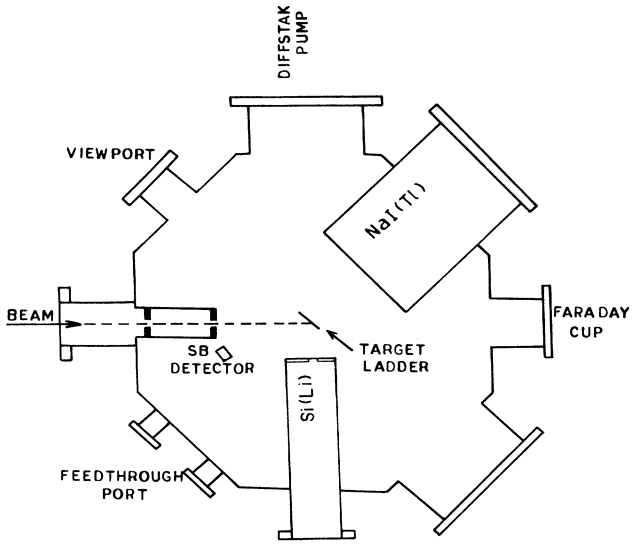

FIG. 3. Schematic diagram of the proton-induced x-ray emission experimental setup.

mm and the beam spot was at the center of this exposed area.

Pulses from the Si(Li) detector preamplifier were fed to an ORTEC-572 model spectroscopy amplifier, the output of which was energy analyzed by a CANBERRA-88 multichannel analyzer. Stability of the electronics was monitored with an ORTEC mercury pulser. Electronic shift was within one channel during the entire period of measurement. The gain of the system was kept at ~ 35 eV/channel. The beam current was adjusted to have the counting rate under the entire spectrum at about 1000 counts/sec. Counting was continued until the counts collected under the $K\beta$ peak were around 10^5 counts.

III. DATA ANALYSIS

All the x-ray spectra were carefully analyzed with the least-squares peak-fitting program of Silin [7]. A fit to the experimental data points was achieved in each case by representing the $K\alpha$ and $K\beta$ peak shapes with Gaussian function by allowing the widths, means, and areas of the calculated peaks and other parameters specifying a quadratic background all to vary in combination until an optimized set was obtained by the method of least squares. The low-energy tail is not included in the fitting as its contribution to the ratio was shown to be quite small [8]. The $K\beta$-to-$K\alpha$ intensity ratios were determined from the fitted peak areas.

IV. CORRECTIONS

Sources of errors contributing to the uncertainty in the measured ratios mainly come from the difference in the $K\alpha$ and $K\beta$ self-attenuations, efficiency correction of the detector, and statistical error. The statistical error contributing to the measured R is calculated by the least-squares fitting program [7]. As far as the correction due to detector efficiency is concerned, it is estimated using the following expression:

$$\epsilon_d(E_X)=e^{-(\mu_{\mathrm{Be}}x_{\mathrm{Be}}+\mu_{\mathrm{Au}}x_{\mathrm{Au}}+\mu_{\mathrm{Si}}\Delta x_{\mathrm{Si}})}(1-e^{-\mu_{\mathrm{Si}}x_{\mathrm{Si}}}) , \tag{1}$$

where μ's are absorption coefficients of the Be window of the Si(Li) detector, the Au layer on the Si(Li) crystal, and the Si(Li) crystal for the detected x rays of energy E_X, and x's are the thicknesses of the Be window, the Au layer, and the Si(Li) crystal. The notation Δx_{Si} represents the thickness of the insensitive region of the Si(Li) crystal. The available data [9] for μ/ρ for different x-ray energies for each of Be, Si, and Au are taken and then interpolated to get the coefficients at other x-ray energies. Using these interpolated μ/ρ values, the efficiency for the Si(Li) detector was calculated for x-ray energies from 4 keV to 30 keV at an interval of 0.2 keV. It was found that the correction due to the Si(Li) detector relative efficiency for R in the x-ray-energy range of present interest is $\leq 1\%$. The intensity ratios are corrected for this relative efficiency.

The main uncertainty in the measured ratios stems from the self-absorption in the target. Since our results for pure metals agree very well with the earlier thin-target results of Slivinsky and Ebert [8] and Paic and Pecar [10], we are confident that our correction for the self-absorption is quite satisfactory. For the γ-ray-fluorescence case, this correction was estimated using the expression

$$R_{\mathrm{corrected}}=\left[\frac{A_\beta}{A_\alpha}\right]R_{\mathrm{measured}} , \tag{2}$$

where

$$\frac{A_\beta}{A_\alpha}=\frac{\dfrac{\mu_\beta}{\cos\theta_1}+\dfrac{\mu}{\cos\theta_2}}{\dfrac{\mu_\alpha}{\cos\theta_1}+\dfrac{\mu}{\cos\theta_2}} \times\frac{\left[1-\exp-\left[\dfrac{\mu_\alpha}{\rho\cos\theta_1}+\dfrac{\mu}{\rho\cos\theta_2}\right]\rho x\right]}{\left[1-\exp-\left[\dfrac{\mu_\beta}{\rho\cos\theta_1}+\dfrac{\mu}{\rho\cos\theta_2}\right]\rho x\right]} . \tag{3}$$

Here ρx corresponds to the thickness of the target in cm^2/g, μ_α and μ_β are attenuation coefficients of the sample for $K\alpha$ and $K\beta$ x rays, respectively, μ is the attenuation coefficient of the sample for 60-keV γ rays, θ_1 is the angle subtended by the Si(Li) detector axis with respect to the normal to the sample surface, and θ_2 is the angle between the incident γ-ray direction and normal to the sample surface (in the present case, $\theta_1=0°$ and $\theta_2=70°$). For thick targets ($x \gg 1/\mu_i$, $i=\alpha,\beta$), one gets

$$\frac{A_\beta}{A_\alpha}=\frac{\dfrac{\mu_\beta}{\cos\theta_1}+\dfrac{\mu}{\cos\theta_2}}{\dfrac{\mu_\alpha}{\cos\theta_1}+\dfrac{\mu}{\cos\theta_2}} . \tag{4}$$

In the case of proton ionization, the self-absorption correction factor is given by

$$\frac{A_\beta}{A_\alpha}=\frac{\int_{E_0}^{0}\sigma_K^I(E)e^{-(\mu_\alpha/\rho)\rho x}\dfrac{dE}{S(E)}}{\int_{E_0}^{0}\sigma_K^I(E)e^{-(\mu_\beta/\rho)\rho x}\dfrac{dE}{S(E)}} , \tag{5}$$

x being given by

$$x=\int_{E_0}^{E}\frac{\cos\theta_3}{\cos\theta_4}\frac{dE}{S(E)}, \tag{6}$$

where θ_3 and θ_4 are the angles subtended by the incident-projectile direction with the axis of the Si(Li) detector and with the normal to the sample surface, respectively (in the present case, $\theta_3=\theta_4=45°$), $S(E)$ is the proton stopping power for the target at proton energy E, E_0 is the incident proton energy, and $\sigma_K^I(E)$ is the K-shell ionization cross section of the target at proton energy E. In our estimation, the absorption coefficients are taken from the tabulated data of Ibers and Hamilton [9], the proton stopping powers are taken from Anderson and Ziegler [11], and the proton ionization cross sections are taken from Cohen and Harrigan [12]. The proton-stopping-power values have uncertainty of about 10%,

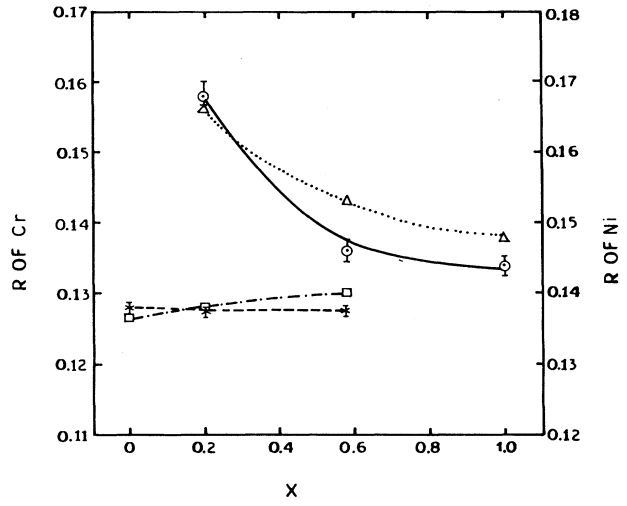

FIG. 4. Comparison of R values of Cr_xNi_{1-x} alloys obtained from γRF [(⊙): Cr; (×): Ni] and PIXE [(△): Cr; (□): Ni] measurements.

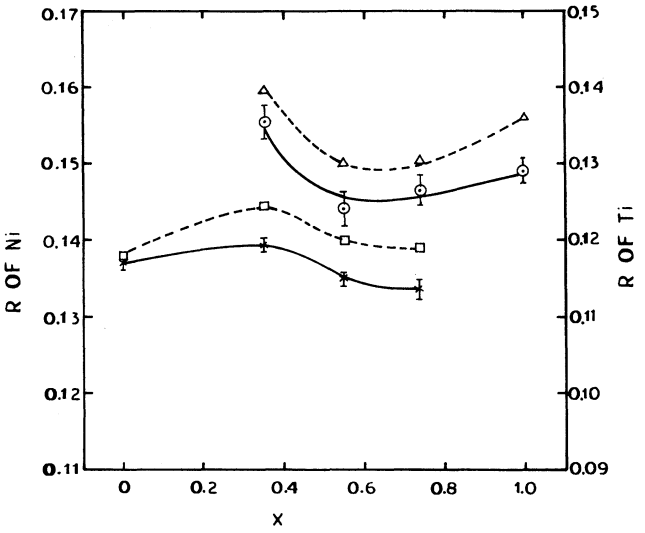

FIG. 5. Comparison of R values of Ti_xNi_{1-x} alloys obtained from γRF [(⊙): Ti; (×): Ni] and PIXE [(△): Ti; (□): Ni] measurements.

which can give rise to $\leq 0.3\%$ error in the corrections for A_β/A_α.

V. RESULTS

The corrected values of R for Cr_xNi_{1-x} alloys obtained from γRF and PIXE measurements are compared in Fig. 4 and both these results are tabulated in Table I. The errors shown are only the statistical errors. These error values do not include the uncertainty in the absorption correction arising from the errors in various mass-attenuation coefficients used for the estimation of the absorption correction and any systematic error in the background correction, especially the PIXE measurements of light targets (Ti and Cr). We expect that this will give rise to an additional uncertainty of 2–4% to our quoted R values. The corrected R values for Ti_xNi_{1-x} alloys obtained from γRF and PIXE measurements are compared in Fig. 5 and both the results are tabulated in Table II.

VI. DISCUSSION

A. For Cr_xNi_{1-x} alloy compositions

As can be seen from Table I and Fig. 4, for certain compositions of Cr_xNi_{1-x} alloys the alloying effects are considerable [1]. In the present work, we have compared the γRF and PIXE results of different alloy compositions. For the sample with 20% chromium concentration, we found about 18% increase in the $K\beta$-to-$K\alpha$ ratio of chromium in γRF measurements; however, we do not find much change in the corresponding nickel value. Increase in the R for chromium could be because of electron transfer from the chromium $3d$ state to the nickel $3d$ state, which was seen in the magnetic studies of Gregory and Moody [3]. Qualitatively, the observed lack of change in the nickel $K\beta$-to-$K\alpha$ ratio and a large change in the chromium ratio could be because there are five $3d$ electrons in Cr, whereas there are more than nine $3d$ electrons in Ni in solid form, so the percentage effect is less for Ni. Most of the theoretical calculations [13,14] so far have taken into consideration only the effect of removal of $3d$ electrons but not addition of electrons to the $3d$ state, and it will be interesting to see what happens in the latter case. The measured increase in the R of the Cr ratio would correspond to removal of about 0.7 electrons [13,14] from its $3d$ orbital. For the composition $x=0.58$, we find only a slight increase in the ratios of both Cr and Ni. Earlier Compton-profile studies [4] for this alloy indicated charge rearrangement between $3d$ and $4s$ states of individual metals, but such a rearrangement appears not

TABLE I. K x-ray intensity ratios R of Cr and Ni in Cr_xNi_{1-x} alloys obtained form γRF and PIXE measurements.

	γRF		PIXE	
x	Cr	Ni	Cr	Ni
0		0.1368±0.0006		0.1380±0.0005
0.20	0.1579±0.0017	0.1383±0.0006	0.1559±0.0009	0.1375±0.0004
0.58	0.1360±0.0016	0.1400±0.0014	0.1436±0.0004	0.1374±0.0005
1.0	0.1338±0.0009		0.1378±0.0005	

TABLE II. K x-ray intensity ratios R of Ti and Ni in Ti_xNi_{1-x} alloys obtained from γRF and PIXE measurements.

	γRF		PIXE	
x	Ti	Ni	Ti	Ni
0		0.1371±0.0006		0.1380±0.0005
0.35	0.1346±0.0022	0.1396±0.0004	0.1397±0.0007	0.1448±0.0003
0.55	0.1240±0.0023	0.1349±0.0005	0.1302±0.0004	0.1403±0.0005
0.74	0.1267±0.0018	0.1335±0.0012	0.1305±0.0003	0.1392±0.0005
1.0	0.1289±0.0014		0.1364±0.0006	

to be producing any appreciable effect on R. The reason for this may be that the valence-state wave function is a hybridization of $3d$ and $4s$ states, and rearrangement of electrons between them does not alter the screening to the $3p$ state. The results for the other compositions that correspond to pure-metal values are found to be in excellent agreement with the compiled data of Salem, Pausossian, and Kreuse [15] and the light-charged-particle data of Li and Watson [2]. They also agree with the theoretical results of Scofield [16] to within 2%.

The PIXE measurements of Cr_xNi_{1-x} alloys support the results obtained from γRF measurements. The small differences seen may be due to uncertainty in the background correction, which is somewhat larger for PIXE data.

B. For Ti_xNi_{1-x} alloy compositions

As can be seen from Table II and Fig. 5, the γRF results of R for Ti in some alloy compositions are higher than that of the elemental-metal results. For $x=0.35$, we find an increase of about 3–4% in the R values of Ti over the elemental-metal value. For Cr_xNi_{1-x} alloys also (see Fig. 4), the percentage increase in R for the concentration around $x=0.35$ is similar to that of Ti in Ti_xNi_{1-x} alloys.

For the alloy composition $x=0.55$, the ratio R is somewhat lower compared to the elemental-metal result, and for the alloy composition $x=0.74$ the ratio is in agreement with the elemental-metal value within the statistical error limits. The PIXE results for Ti indicate higher values of R as compared to the results of the γRF measurement. Previous high-resolution x-ray spectroscopy studies in Ti by Hill *et al.* [17] gave the evidence of formation of simultaneous L- and M-shell vacancies, along with the K vacancy whose intensity falls off with the increase of proton energy. The work of Li, Watson, and Hansen [18], however, demonstrated that for thick samples the R value decreases due to the effect of critical self-absorption of $K\beta$ x ray. Our present study, however, shows that the $K\beta$-to-$K\alpha$ ratios for Ti of PIXE measurements are higher than the γRF results for all alloy compositions. A plausible explanation for this could be that, because of the larger background in the PIXE experiments, the background correction is giving rise to some systematic error in the evaluation of the ratio R.

We have also observed a small increase in the R values of nickel in the PIXE measurements, which could be again because of uncertainty in the background correction. The R value of Ni is not found to change much with alloy composition, which may be because the percentage change in the number of $3d$ electrons of nickel due to alloying is small, so the percentage effect in R is less for Ni.

We tried to see if the observed increase in R for the case of dilute alloys could be due to secondary excitation of Ti and Cr from nickel x ray, but this process, we think, is not going to affect the value of R, although there will be a general increase in the x-ray yield.

In conclusion, we would like to say that measurement of the $K\beta$-to-$K\alpha$ intensity ratios can be a sensitive probe in studying the charge-transfer effect in alloys. Although a qualitative explanation of the present findings can be given through charge-transfer or -rearrangement models, a calculation based on different initial electronic configurations of the atom in the alloy would be more useful in interpreting the present data.

ACKNOWLEDGMENTS

The authors thank Mr. R. K. Yadav for his assistance during the experiments. Our gratitude goes to the operation staff of the 9SDH-2 tandem pelletron accelerator, and in particular to Dr. D. P. Mahapatra, Mr. R. C. Nayak, and Mr. Anup Behera for their help in various stages of the experiment with the proton beam.

[1] C. R. Bhuinya and H. C. Padhi, Institute of Physics, Bhubaneswar (India) Report No. 91-41.
[2] T. K Li and R. L. Watson, Phys. Rev. A **9**, 1574 (1974).
[3] I. P. Gregory and D. E. Moody, J. Phys. F **5**, 36 (1975).
[4] D. Pal and H. C. Padhi, Physica Status Solidi B (to be published).
[5] D. Pal and H. C. Padhi, Philos. Mag. B **65**, 553 (1992), and references therein.
[6] C. R. Bhuinya and H. C. Padhi, Institute of Physics (India) Report No. 91-52.
[7] I. Silin, CERN Computer Centre Library Programme No. D510 (1971).
[8] V. W. Slivinsky and P. J. Ebert, Phys. Rev. A **5**, 1681 91971).
[9] J. H. Hubbel, W. H. McMaster, N. K. Del Grande and J. H. Hamellett, in *International Tables for X-ray Crystallography,* edited by J. A. Ibers and W. C. Hamilton (Keynoch, Birmingham, 1974), Vol. 4, p. 47.

[10] G. Paic and V. Pecar, Phys. Rev. A **14**, 2140 (1976).
[11] H. H. Anderson and J. F. Ziegler, *Hydrogen Stopping Powers and Ranges in all Elements* (Plenum, New York 1977).
[12] D. D. Cohen and M. Harrigan, At. Data Nucl. Data Tables **33**, 255 (1985).
[13] E. Arndt and E. Hartmann, Phys. Lett. A **83**, 164 (1981).
[14] E. Arndt, G. Brunner, and E. Hartman, J. Phys. B **15**, L887 (1982).
[15] S. I. Salem, S. L. Pausossian, and R. A. Kreuse, At. Data Nucl. Data Tables **14**, 92 (1974).
[16] J. S. Scofield, Phys. Rev. A **9**, 1041 (1974).
[17] K. W. Hill, B. L. Doyle, S. M. Shaforth, D. H. Madison, and R. D. Deslattes, Phys. Rev. **13**, 1334 (1976).
[18] T. K. Li, R. L. Watson, and J. S. Hansen, Phys. Rev. A **8**, 1258 (1973).